Indian J. Vet. Pathol., 49(1) : 38-48, 2025: DOI: https://doi.org/10.5958/y870gp74

RESEARCH ARTICLE

Studies on the pathomorphology of epidemics of Infectious Bursal Disease (IBD) in chicken

B.C. Girish*, K. Sujatha[1], H.D. Narayanaswamy[2], K. Nagappa[3], D. Ramesh[4] and M. Bindu[5]
Department of Veterinary Pathology, Veterinary College, Hassan, KVAFSU, Karnataka, [1]Centre for Continuing Veterinary Education and Communication, College of Veterinary Science, Tirupati, [2]Department of Veterinary Pathology, Veterinary College, Hebbal, [3]Department of Veterinary Public Health and Epidemiology, [4]Department of Veterinary Physiology and Biochemistry, [5]Affigenix Biosolutions Ltd, Hebbagodi, Bengaluru, India

Address for Correspondence
B.C. Girish, Associate Professor, Department of Veterinary Pathology, Veterinary College, Hassan, KVAFSU, Karnataka, India, E-mail: girishhouse@gmail.com

Received: 12.11.2024; Accepted: 26.12.2024

ABSTRACT

Viral pathogens induce distress in poultry and economic loss to farmers worldwide. Infectious Bursal Disease (IBD), a Birna viral immunosuppressive infection of poultry continues to affect birds including regions of Karnataka and neighbouring states; hence study on IBD was undertaken with the objective to estimate its prevalence and understand its pathology. Data from 15 IBD outbreaks from commercial broilers (11) and layers (2) as well as native birds (2) showed average morbidity of 29.3% (7.1 to 100%) and mortality of 18.4% (7.5 to 100%). Maximum number of 9 outbreaks was recorded in the age groups 1-4 weeks accounting for 60 percent of the total outbreaks and the same age group also showed highest morbidity (Average 33.1%, Range: 9-100%) and mortality (Average 22.4%, Range: 7.5-100%). Affected birds showed vascular and atrophic changes in lymphoid organs with secondary changes in liver, kidneys and skeletal muscles. Ultrastructural studies of thymus revealed severe necrosis and increased electron density in lymphocytes and hyperplasia of reticular cells. Bursa also revealed areas of lymphocytic apoptosis and engulfed phagocytic bodies in these macrophages. The cytoplasmic granules of bursal secretory dendritic cell (BSDC) had fused together, forming big, irregularly shaped, electron dense bodies. Amplification of VP2 gene using reverse transcriptase PCR showed 319 bp products having phylogenetic similarity to Indian isolates. Eight IBD outbreaks showed concurrent infection with other pathogens. The bioinformatic analysis of VP-2 protein suggested the presence of the glycine like amino acids predominant in the alpha helical secondary structure.

Keywords: Bursa of Fabricius, epidemics, PCR, RNA Virus

INTRODUCTION

A healthy immune system is vital for effective poultry production. Any factor that causes dysfunction of humoral and cellular immune system will certainly result in poor vaccination response, production and economic losses and flaring up of opportunistic pathogens. Viral pathogens can cause huge economic losses in poultry farms worldwide including immunosuppression[1-4]. The important viral agents that cause immunosuppression include Marek's disease virus (MDV), Chicken infectious anemia virus (CIAV), Infectious Bursal Disease virus (IBDV), Reovirus, Avian Leukosis virus, reticuloendotheliosis, Newcastle disease virus and Avian Influenza virus[1,5-6].

Infectious Bursal Disease (IBD) is a highly contagious and acute immunosuppressive disease of young chickens and is caused by Birna virus. The disease is characterized by severe immunosuppression leading to secondary bacterial infections and dermatitis, adenoviral infections and failure of vaccinations[7]. The immunosuppression seen in IBD is complex involving depletion of B cells by apoptosis and also inhibiting innate immune response directly[8]. Infectious Bursal Disease (IBD) targets the chicken's immune system in a very comprehensive and complex manner by destroying B lymphocytes, attracting T cells and activating macrophages[9]. It has been noted that IBDV and RNA virus has a high mutation rate and can give rise to viruses with altered antigenicity and increased virulence[10-11] and the re-emergence of IBD with antigenic variants and highly virulent strains had been the reason for significant losses and high mortality. IBD affected birds had elevated mortality rates, bursal atrophy, poorer feed conversion ratio (FCR) and reduced meat production[12].

How to cite this article : Girish, B.C., Sujatha, K., Narayanaswamy, H.D., Nagappa, K., Ramesh, D. and Bindu, M. 2025. Studies on the pathomorphology of epidemics of Infectious Bursal Disease (IBD) in chicken. Indian J. Vet. Pathol., 49(1) : 38-48.

Pathogenesis of the disease is complex involving both humoral and cellular immune responses being compromised by IBD virus; Inhibition of the humoral immunity could be attributed to the destruction of immunoglobulin-producing cells by the virus[13]. VP1 is the viral RNA dependent RNA polymerase while VP2 is the major host-protective immunogen carrying

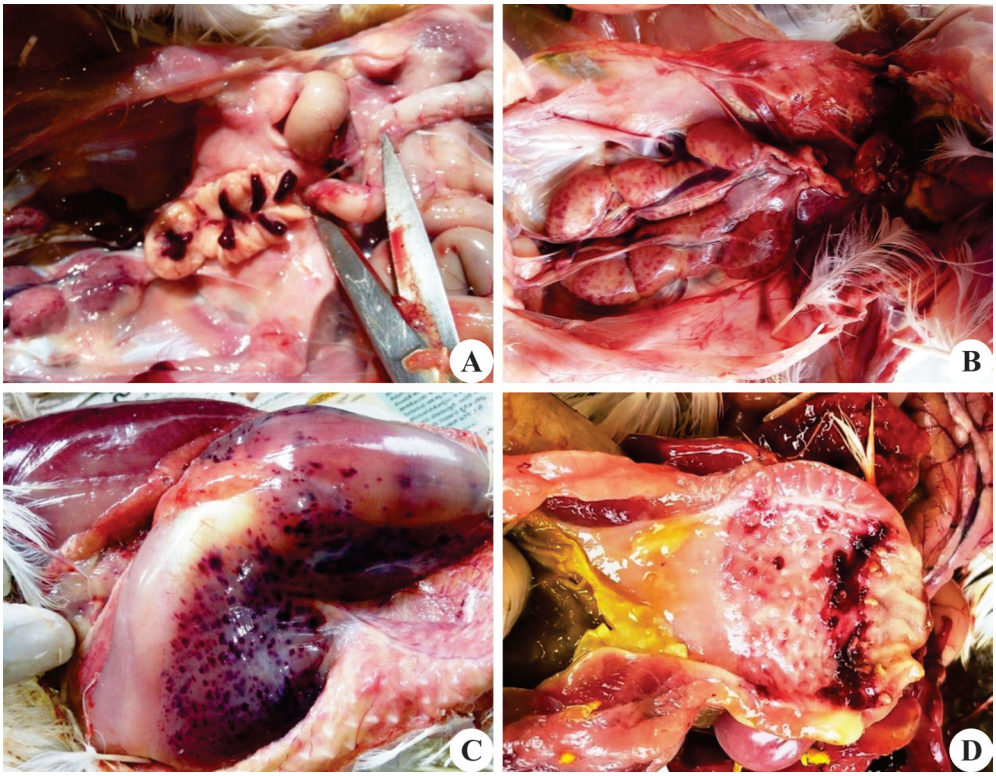

Fig. 1. Gross pathological changes in organs of chicken affected with IBDV. **A.** Bursa: Multiple extensive hemorrhages and hemorrhagic exudate. **B.** Kidney: Hemorrhages and mottled appearance in a broiler chick. **C.** Dorsal view of thigh muscles showing severe multifocal petechial to ecchymotic hemorrhages. **D.** Proventriculus: Hemorrhages prominently visible at the junction with gizzard.

all neutralizing epitopes some of which are responsible for antigenic variation[14]. It has been observed that classical and vvIBD virus induces differential host immune responses by up regulating the expression of Th1-like and pro-inflammatory cytokines such as IL-12, IFN-γ, IL-1β, IL-6, iNOS and IL-18 in bursa[11]. It is recorded that Bursa of Fabricius is the principal diagnostic organ in birds that died during the acute phase of vvIBD[7]. Various immunological and molecular diagnostic methods have been described for the confirmation of the disease[11,15-19]. Clinical presentation of the diseases varies according to the strain involved. The variant IBDV strains normally cause subclinical infection in chickens. The classical IBD viral strains can cause clinical signs of disease and moderate mortality rates whereas vvIBDV strains are known to cause high mortality rates[11-12].

The current study was carried out in Karnataka and neighbouring southern states of India with the objectives of studying prevalence and pathology of Infectious Bursal Disease (IBD) with special emphasis on lymphoid organs of chickens, characterizing the ultra-structural changes in such organs and characterizing the disease by molecular techniques.

MATERIALS AND METHODS

Sample collection

The study was carried out in the Department of Veterinary Pathology, College of Veterinary Science, Sri Venkateshwara Veterinary University, Tirupati and Department of Veterinary Pathology, Veterinary College, Hassan of Karnataka Veterinary Animal and Fisheries Sciences University between January 2017 and August 2022. Poultry farms in southern districts of Karnataka and neighbouring states including Andhra Pradesh and Tamil Nadu presenting outbreaks of IBD formed the basis of sample collection in the study.

Flock history and clinical signs

Detailed information on the farm outbreak with respect to type of birds (broiler, layer, breeder or country birds), flock strength, breed/strain details, age, source of feed and water, production performance, type of litter, vaccination details, morbidity, mortality, clinical signs, previous history of outbreak and any other necessary details were collected.

Necropsy examination and collection of biological samples

Detailed necropsy examination was undertaken. Internal examination of body cavities, visceral organs and lymphoid organs was carried out and all visible gross lesions were systematically recorded. Tissue impression smears were collected. Tissue samples from all vital organs and lymphoid organs were collected

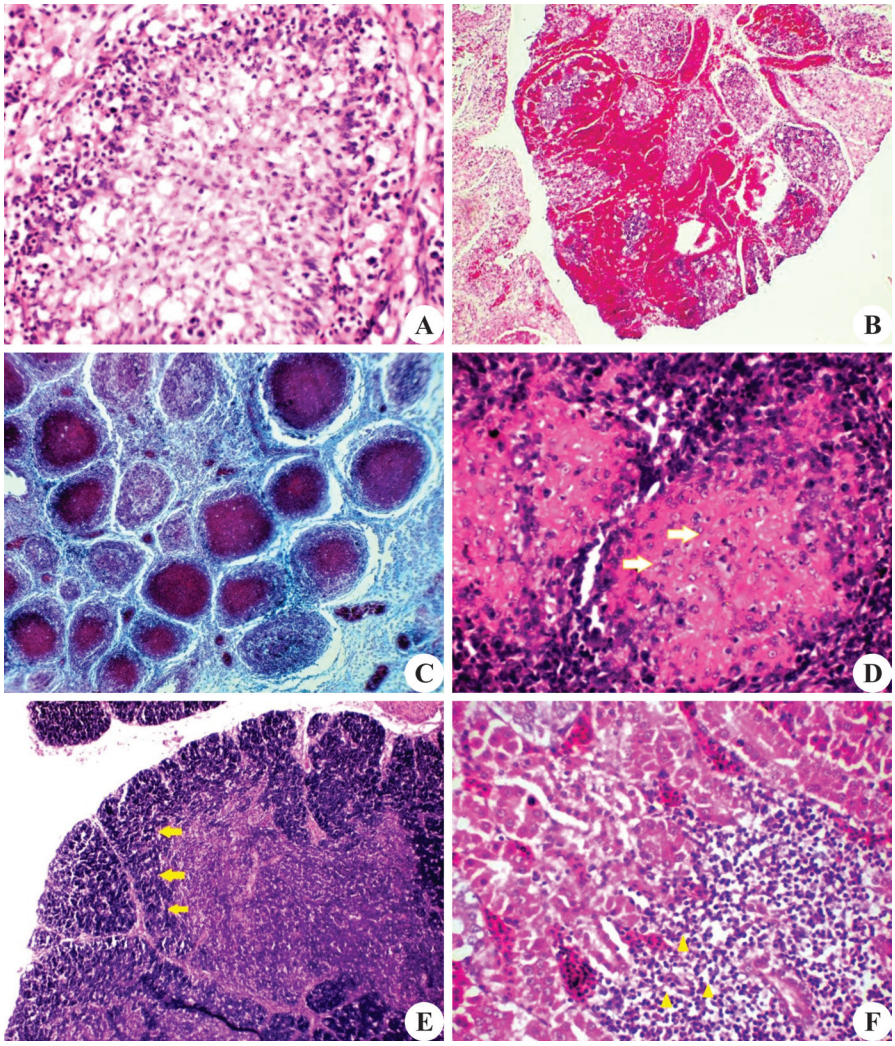

Fig. 2. Histopathological changes in organs of chicken affected with IBDV. **A.** Bursa of Fabricius: Severe depletion of lymphocytes indicated by hypocellularity and necrotic changes such as pyknosis and karyorrhexis and karyolysis of lymphocytes (H&E x400). **B.** Bursa of Fabricius: Severe hemorrhages and congestion inside and surrounding the atrophied follicles (H&E x100). **C.** Bursa of Fabricius: Extensive fibroplasia evident by proliferation of blue colored collagen fibres (Masson's x100). **D.** Spleen: Necrotic changes in the germinal follicles and the periarteriolar lymphoid sheath with proliferation of reticulo-epithelial cells (H&E x100). **E.** Thymus: Atrophy and thinning of the cortex with lymphocytolytic changes (H&E x100). **F.** Kidney: Heterophilic infiltration and nephritic area in the interstitium (H&E x400).

and preserved in 10% neutral buffered formalin for histopathological examination. The representative tissue samples were also collected for PCR in a sterilized labelled tissue sample bottles and were stored at -20^{O}C immediately.

Microbiological and histopathological examination

The samples collected aseptically during necropsy examination were used to investigate the concurrent bacterial infection as per the standard protocols. The impression smears of various vital organs during necropsy examination were air dried and fixed with absolute methanol for 5 minutes and stained with diluted Giemsa stain (1:10 V/V) for 20 minutes.

Tissue samples for histopathological examination were processed by routine paraffin embedding technique and sectioned at five micron thickness. The sections were stained with routine Hematoxylin and Eosin (H&E) method. Special stains such as Masson's Trichrome or Van Gieson (Connective tissue) and Perl's Prussian blue stain (Hemosiderin pigments) were used on need basis[20]. Tissue morphometric evaluation for measuring the diameter of the bursal follicle was done using a validated software TC Capture version 3.9 (build 5001). The average values of 5-6 bursal follicles in age matched birds was carried out for minimum of 6 birds and average was calculated for comparison.

Electron microscopy

Tissue samples from lymphoid organs were fixed in 2.5% glutaraldehyde in 0.1M Phosphate buffer (pH 7.2) for minimum of 24 hours at 4^{O}C. Further, post fixed

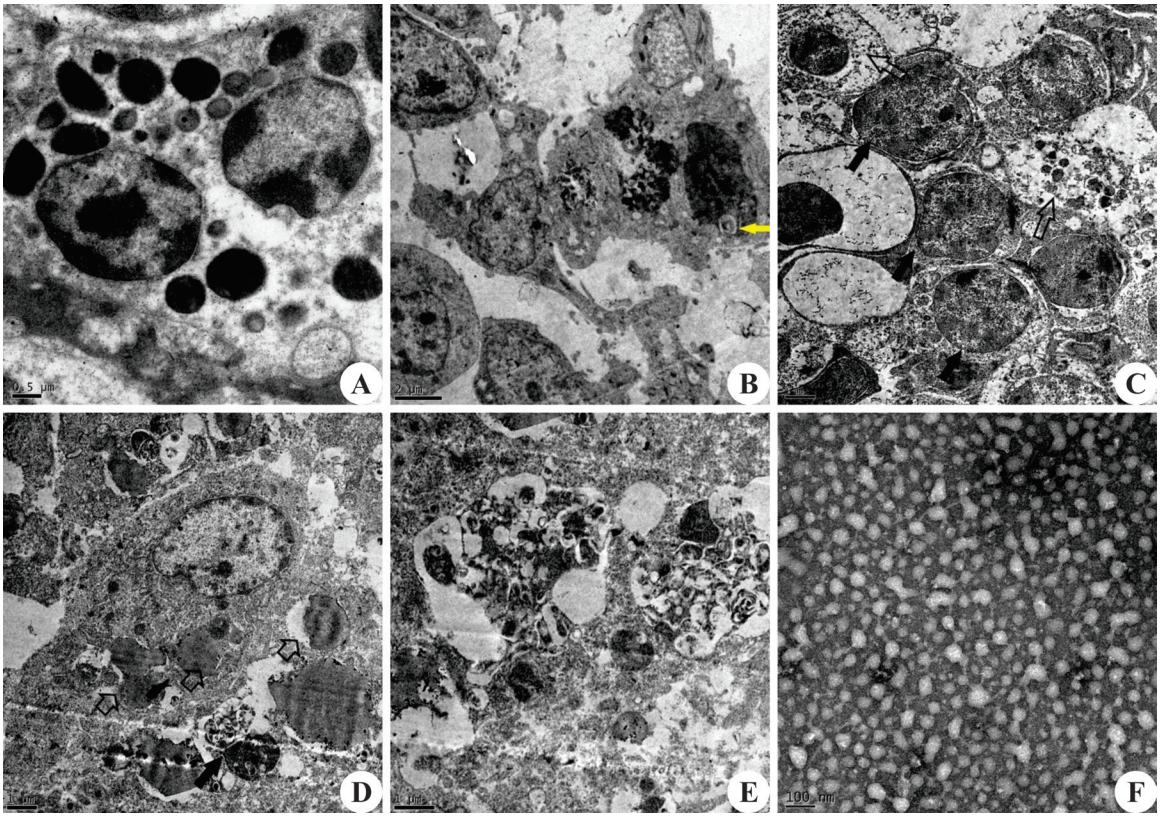

Fig. 3. Ultrastructural changes in organs of chicken affected with IBDV. **A.** Thymus: Nuclei and cytoplasm of lymphocytes showed increased electron density (Uranyl Acetate). **B.** Thymus: Lymphocytes with myelin figures (Uranyl Acetate). **C.** Thymus: Necrotic changes of the lymphocytes shown by light arrow and hyperplasia of the reticular cells indicated by dark arrow (Uranyl Acetate). **D.** Bursa of Fabricius: Note the necrotic areas with nuclear changes such as karyorhexis (Dark arrow) and karyolysed fragments (Light arrow) of lymphocytes (Uranyl Acetate). **E.** Bursa of Fabricius: Bursal secretory dendritic cell (BSDC) forming big and irregularly shaped electron dense bodies (Uranyl Acetate). **F.** Single-shelled non-enveloped IBD virions with icosahedral symmetry and a diameter of around 50 nm (Uranyl Acetate).

in aqueous osmium tetroxide for 3 hours and washed with deionized distilled water, dehydrated in series of graded alcohols, infiltrated and embedded in araldite resin. It was incubated at 80^{O}C for 72 hours for complete polymerization. Ultra-thin (60 nm) sections were made with a glass knife on ultra-microtome (Leica Ultra cut UCT-GA-D/E-1/00), mounted on copper grids and stained with saturated aqueous Uranyl acetate (UA) and counter stained with Reynolds lead citrate (LC). Viral suspension was prepared from the tissues of the affected birds. Copper grids (Carbon coated) were glow discharged for 30 seconds using polaron carbon evaporator. 5µl of sample was loaded on the glow discharged grids and allowed to dry for 10 minutes. 5µl of 2% Uranyl acetate was loaded on the grids for 30 seconds and excess was wiped off by using Whatman filter paper and allowed to dry. Samples were loaded on the TEM single tilt Holder, loaded into TEM. Further, they were finally imaged and analyzed at 120 kv[21].

Molecular characterization

RNA was extracted from the samples using Trisol (GeNei™ TRIsoln) method and cDNA was synthesized using TAKARA Kit. The temperature and time combination was 37^{O}C, 85^{O}C and 4^{O}C for 15 minute (priming), 5 seconds (Reverse transcription), for infinity (optional) respectively. cDNA synthesized thus was stored at -20^{O}C for long term storage.

Primers were designed to amplify VP2 gene which codes for VP2 protein, the major host-protective protein of IBD Virus. Primers were synthesized and procured commercially from M/s Bio Serve Biotechnologies (India) Pvt. Ltd., Hyderabad. They were reconstituted in 1x TE buffer (TE) to obtain the required concentration of 100 picomol/µL. The sequences of the primers used was 5′-ATGCTCCAGATGGGGTACTTC- 3′ (IF) and 5′-TTGGACCCGGTGTTCACG- 3′ (IVIR) to target the product size of 319 bp.

PCR cycling conditions for cDNA amplification included Initial denaturation with 95^{O}C for 3 minutes, 35 cycles of denaturation (94^{O}C for 1 minute), annealing (48^{O}C for 1 minute) and extension (72^{O}C for 2 minutes) followed by final extension (72^{O}C for 5 minutes). DNA confirmation was carried out by 1.5% Agarose gel

electrophoresis following visualization and capturing of the images by Image Lab Software (Version 5.1, Bio-Rad Laboratories Inc). Sequencing (Eurofins Genomics India Pvt. Ltd.) was done to identify the degree of homology using the final amplicons and phylogenetic tree was constructed.

Bioinformatic Analysis of IBD-VP2

The 3D structure of the VP2 with predicted protein sequence was drawn using SWISS PROT expasy platform. GMQE (Global Model Quality Estimate), a quality estimate which combines properties from the target-template alignment and the template structure was used to calculate the overall model quality measurement between 0 and 1. The QMEAN z-score in SWISS-MODEL was used to measure of how close the model is to structures of a similar size that were obtained experimentally. Structural assessment was made using Ramachandran plot.

RESULTS

Epidemiological findings

A total of 15 outbreaks were documented that included 11 outbreaks from broiler birds, 2 from non-descript birds and 2 from commercial layers. Total number of birds investigated was 298 (average of 19.87 birds per outbreak in 15 outbreaks). Out of these 15 outbreaks, maximum number of 9 outbreaks was recorded in the age groups 1-4 weeks accounting for 60 percent of the total outbreaks. In this, 7 cases (46.7%) were recorded between 3-4 weeks, making it the most susceptible age. This was followed by 5 outbreaks from age group 5-8 weeks (33.3%) and one case from age group 9-12 weeks (6.7%).

The average morbidity and mortality of 15 flocks were 29.3% (Range: 7.1 to 100%) and 18.4% (Range: 7.5 to 100%) respectively. Maximum morbidity (Average 31.4%) was seen in broilers followed by indigenous birds and layers. Highest mortality (Average 31.4%) was seen in broiler birds followed by country birds and layers. Highest morbidity was recorded in the age group 1-4 weeks (Average 33.1%, Range: 9-100%) and highest mortality was also found in the same group (Average 22.4%, Range: 7.5-100%).

Clinical signs

The affected birds initially showed trembling followed by yellowish white or greenish watery diarrhea. This was followed by dullness, depression, anorexia, ataxia, ruffled feathers, soiled vent, prostration, closed eyes, decreased water consumption and sudden death. Birds affected with IBD exhibited lateral recumbency and dyspnea before succumbing to death. Few birds also exhibited bloody discharge from cloaca. Mortality was noticed 2-3 days after appearance of first clinical sign and peaked at 4-5 days. In one flock that had concurrent infection with ND the birds exhibited severe emaciation, neurological signs and greenish diarrhea.

Gross pathology

In acute phase of disease bursa from infected birds was swollen and edematous. The enlarged bursa showed multiple hemorrhages (Fig. 1A) and necrotic foci in the follicles and presence of gelatinous inflammatory fluid surrounding the bursa. In the chronic phase the changes included greyish brown discoloration and atrophied bursa with presence of cheesy material. Spleen of few birds exhibited minimal decrease in the size due to atrophic changes with congestion and mottling. Thymus, cecal tonsils and bone marrow revealed hemorrhages, atrophy and congestion in few affected birds in acute phase of the disease. Kidneys showed nephrotic changes characterized by congestion, mottling, enlargement (Fig. 1B) and hemorrhages along with distension of ureters with whitish uric acid crystals in around 40% of the birds. Birds with kidney lesions correlated well with severe dehydrative changes. Few percentage of birds (10-15%) showed multifocal necrosis on the liver and they appeared enlarged and dark brownish. IBD affected birds also showed moderate to severe petechial and ecchymotic hemorrhages on pectoral and thigh muscles (Fig. 1C). In majority of the birds, ecchymotic hemorrhages in the mucosa of the proventriculus mainly at the junction with esophagus (Fig. 1D) and gizzard were observed. Occasionally, mucosal hemorrhages were also seen in the gizzard. Few affected birds also exhibited mucosal erosions and congestion in the small intestine.

Histopathology

Lymphoid organs: Bursa of Fabricius in acute phase of the disease showed severe depletion of lymphocytes

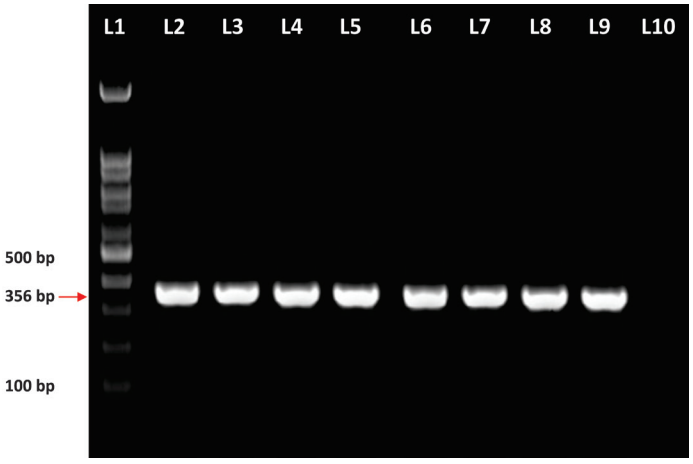

Fig. 4. Agarose gel electrophoresis image showing amplification of 319 bp PCR product in samples specific to VP2 gene of IBDV. L1: 100 bp DNA Ladder, L2: Sample ND1, L3: Sample ND2, L4: Sample ND3, L5: Sample ND4, L6: Sample ND5, L7: Sample ND6, L8: Sample ND7, L9: Sample ND8, L10: No template control.

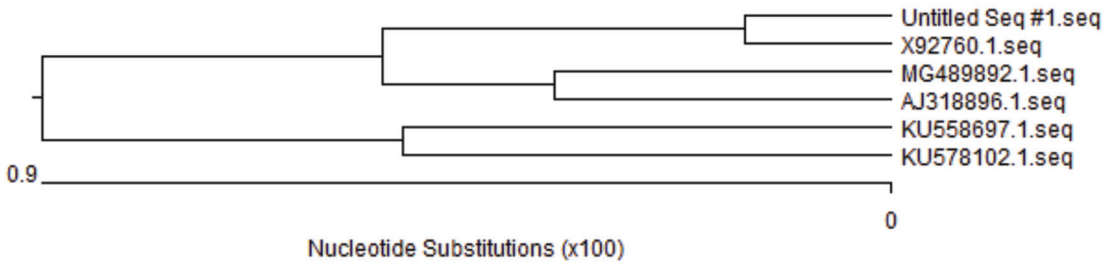

Fig. 5. Dendrogram of partial sequence of VP2 gene of IBDV showing phylogenetic relationship of field IBDV with other reported strains.

indicated by hypocellularity and multiple cystic spaces in both medulla and cortex. Many follicles in the affected birds showed necrotic tissue debris with nuclear changes involving pyknosis and karyorrhexis and karyolysis of lymphocytes (Fig. 2A). Moderate to severe hemorrhages and congestion in the follicles was also recorded more often (Fig. 2B). Birds in the post outbreak stage showed cystic cavities in the place of follicular medullary areas. There was an increase and decrease in the diameter of follicles in acute and chronic phase respectively. The mean diameter in the affected birds was 516µ in the acute phase of the disease and 214µm in the chronic phase compared to 450µ in the age matched disease free birds. Extensive fibroplasia was also evident with proliferation of collagen in the interfollicular areas (Fig. 2C). Occasionally bursal epithelial cells formed glandular appearance with mucin like material.

Spleen in acute phase of the infection showed moderate vascular changes accompanied by histiocytosis, heterophil infiltration and lymphocytolysis (Fig. 2D). In the chronic phase regenerating change was seen in the form of secondary lymphoid follicles by proliferating lymphoblasts. In the thymus, atrophy of the cortex was noticed with lymphocytolysis in small percentage of birds (Fig. 2E). This was coupled with hypertrophy of epithelial reticular cells and mild decrease in lymphocytic numbers in the medulla and increase in the number of tingible body macrophages leading to starry sky appearance of the cortex. Cecal tonsils revealed lymphoid cell necrosis leading to hypocellularity of lymphoid cells. Additionally, infiltration of heterophils and macrophages, multifocal hemorrhages, degenerative changes of reticular cells were recorded. Bone marrow revealed hypocellularity of hematopoietic cells, decrease in the number of granulocytes and agranulocytes and increased numbers of macrophages. Plasma cell population was decreased in the Harderian glands.

Non-lymphoid/Other vital organs: Cortex of the kidneys revealed moderate to severe congestion accompanied with vacuolar degeneration of the convoluted tubules. Few tubules showed eosinophilic hyaline like proteinaceous material along with infiltration of lymphocytes and mononuclear cells (Fig. 2F). Few areas of haemorrhages with heterophils infiltration and nephritic areas were also recorded in the interstitium. Livers of affected birds showed vacuolar degeneration, hyperplastic changes and perivascular infiltration of mononuclear cells and congestion of sinusoids and surrounding area of central vein and occasionally disruption of hepatic cords with lymphocytic infiltration.

Moderate to severe hemorrhages and disruption of plical architecture were noticed in the proventriculus. Similarly, mild to moderate haemorrhages in between cardiac muscles with occasional myocarditis in heart and moderate hemorrhages were recorded in skeletal muscles of thigh and pectoral area with lymphocytic infiltration. Lungs revealed congestion, haemorrhages and oedematous changes.

Ultrastructural changes

Thymus revealed severe necrosis of the lymphocytes and hyperplasia of the reticular cells. Nuclei and cytoplasm of lymphocytes showed increased electron density (Fig. 3A) and myelin figures (Fig. 3B). Reticular cells appearing dark and small with distinct cytoplasmic contents were found to be relatively increased (Fig. 3C). Lymphocyte numbers appeared decreased. Granulocytes mainly heterophils were relatively more. The normal lymphocytes, dendritic cells, macrophages, heterophils, plasma cells, endothelial cells, erythrocytes and abundant reticular cells were observed with no major pathological observations in the spleen.

Relative decrease in the number of lymphocytes and increase in macrophage like cells (mal) was observed in the Bursa of Fabricius (Fig. 3D). TEM revealed areas of lymphocytic apoptosis and engulfed phagocytic bodies within macrophages. The cytoplasmic granules of bursal secretory dendritic cell (BSDC) was fused together, forming big, irregularly shaped, electron dense bodies (Fig. 3E). A fine-flocculated discharge substance was found surrounding these cells. Few necrotic areas with nuclear changes such as karyorrhexis and karyolysis were also recorded. The virus particles single-shelled, non-enveloped virion with icosahedral symmetry and a diameter of around 50 nm were observed in negative staining preparations (Fig. 3F).

Molecular confirmation

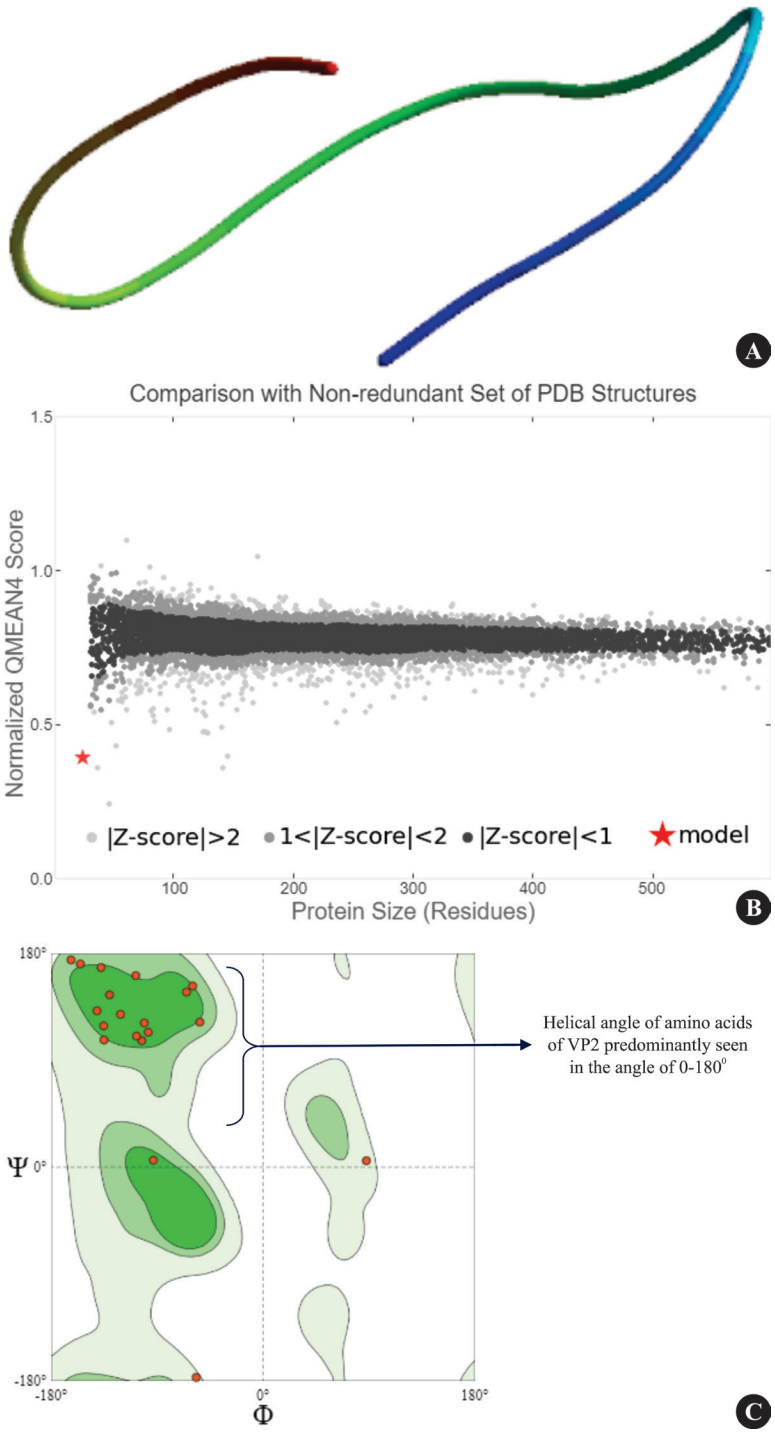

Fig. 6. Bioinformatic Analysis of IBD-VP2. **A.** 3D structure of VP2 in SWISS PROT. **B.** Normalized QMEAN score plot. **C.** Ramachandran plot showing secondary structure of VP2 protein.

Mixed tissue samples from the affected birds were subjected to RNA isolation using Trisol (GeNei™ TRIsoln) kit. The RNA obtained was used for cDNA synthesis employing TAKARA Kits. The RT-PCR was adopted for the detection of IBD antigen for the specific amplification of 319 bp product corresponding to variable region of VP2 gene of IBD virus (Fig. 4). IBD positivity was recorded in all 15 flock outbreaks.

The amplicons obtained by PCR reaction of VP2 gene from samples IBD were subjected to sequence analysis. The 319 bp product was sequenced and phylogenetic tree was drawn and similarity in terms of percentage between various isolates was presented (Fig. 5). This revealed 98 to 100% similarity of strain isolated in this study with

Infectious Bursal Disease virus gene for VP5 protein and VP2-4-3 polyprotein, genomic RNA, IBD virus gene for polyprotein, mutant IBD virus strain AvvBvv segment A and other two indian isolates.

Concurrent infection

Eight outbreaks showed concurrent infection with *E. coli* (4), Salmonellosis (1), CRD (1), Aflatoxicosis (1), Newcastle disease (1) and mixed bacterial infection leading to enteritis (1). The average morbidity and mortality in the outbreaks with concurrent infection were 27.1 and 43.5% respectively. These values in outbreaks without concurrent infection were 12.6 and 19.8% that indicated higher morbidity and mortality in the former group by 14.5 and 23.7%.

The microscopic pathological changes in concurrent infection with *E. coli*, Salmonellosis, CRD, Aflatoxicosis, ND and mixed bacterial enteritis were consistent with the usual pattern of lesions observed in these conditions and correlated well with gross observations. *E. coli* infection revealed fibrinous pericarditis and perihepatitis. The birds with Fowl cholera showed multifocal necrotic areas in the liver with heterophil infiltration and presence of bipolar gram negative organisms in the impression smears of various organs. Birds with Chronic respiratory disease (CRD) showed fibrinopurulent exudate in trachea and lungs. Mixed bacterial enteritis showed presence of many types of bacteria with multiple morphology and heterophil infiltration and concurrent aflatoxicosis was characterized by severe fatty change and multifocal necrosis in the liver.

Bioinformatic Analysis of IBD-VP2

The structural analysis of the IBD-VP2 protein using the SWISS PROT with 3D structure of VP2 and predicted protein sequence is presented in Fig. 6A. This suggested that VP2 of IBD is a manomeric protein with 99 amino acids. The GMQE score of the IBD-VP2 was 0.07. The "QMEAN" score, which is based on the linear combination of four statistical potentials of mean force, was used. Using Z-scores of four as in Fig. 6B and a total of 5 were contrasted with empirically determined structures of comparable size. Ramachandran plot (Fig. 6C) suggested the presence of the glycine like amino acid predominant in the alpha helical structure of the protein.

DISCUSSION

Viral immunosuppressive diseases are economically more important as they cause severe mortalities and loss to the farmers. Also, it makes the birds susceptible for other concurrent bacterial infections further worsening the condition[1-2].

A total of 15 outbreaks of IBD were recorded in the current study. The prevalence of this in Broilers, Layers and Non-descript/desi birds was 11, 2 and 2 respectively. Its prevalence in poultry has been described in India[22-24] and globally[6,11,25-26]. Further it is matter of concern that the re-emergence of IBD with antigenic variants and highly virulent strains that has led to significant losses to poultry farmers[26]. Maximum occurrence of 60% of IBD was recorded in the age group 1-4 weeks. In this, 7 cases (46.7%) were recorded between 3-4 weeks, making it the most susceptible age followed by 5-8 weeks that showed 33.3% similar to previous observations[23-24]. The early age susceptibility might be due to the size of the bursa in early phase of life is regarded as influencing factor for higher incidence of the disease in young chicks less than 4 weeks old[23] and broiler and breeder vaccination programs are not effective for controlling variant IBD infections[12].

The morbidity and mortality in IBD were 29.3% (Range: 7.1 to 100%) and 18.4% (Range: 7.5 to 100%) respectively. Maximum morbidity (Average 31.4%) and mortality (Average 20.5%) has been recorded in broilers. Highest morbidity was recorded in the age group 1-4 weeks in line with the previous findings[24,27,28]. Morbidity and mortality touching even 100% could also be due to culling of the entire bird stock by the farmers where birds do not show any signs of recovery in spite of attempted treatment for secondary bacterial infections. Backyard chicken flocks apart from getting clinical disease can also serve as a reservoir for these viruses and may be playing a role in their dissemination[28].

The symptomology observed in IBD was in tune with the previous findings[18,28-31]. Most of the outbreaks were of acute progressive clinical form associated with Asian/European strains and showed varying severity mostly linked to differing age, sensitivity and vaccination status[29]. The outbreaks recorded in the current study even in vaccinated flocks draw considerable support[11] who observe that vaccination though is the most important measure to control IBD, extensive usage of live vaccines is encouraging evolution of new strains resulting in outbreaks around the globe.

The gross changes in bursa and lymphoid organs might be due to the proven fact that IBDV targets the chicken's immune system in a very comprehensive and complex manner by destroying B lymphocytes, attracting T cells and activating macrophages[9]. It is also noted that the massive destruction of bursal follicles and lack of regeneration process leading to chronic immunosuppression and further complication[10]. The immunosuppressive changes in thymus and spleen have been recorded in both experimental[30,32] and natural outbreaks[24,31,33,34]. No significant change observed in the post outbreak period was probably due to reparative/ healing processes. The reason change in kidneys was probably linked to severe dehydration[35]. The concurrent infections draw significant resemblance with the observations made by previous workers[36,37]. Further, it

is stated that IBD plays a triggering role in *E. coli* and *Mycoplasma gallisepticum* induced respiratory disease complex in broilers[36]. The concurrent infections in present study might be due to immunosuppression and vaccine failure[38].

The histopathological observations in bursa of acutely affected birds were as per the previous observations made[24,27,30,33,34,39,40]. The morphometric changes in the bursal diameter might be due to vascular changes in the acute inflammation (increased) and atrophy in chronic inflammation (decreased). These changes might be due to replication of IBD virus in immature B lymphocytes that are considered as target for the virus. Hence, these changes are anticipated in bursa and other lymphoid organs. Necrotic changes noticed in the germinal follicles and the periarteriolar lymphoid sheath and proliferation in the post outbreak phase due to chronic exposure of spleen was in accordance with the earlier observation[41]. Microscopic changes noted in thymus, bone marrow and cecal tonsils were similar to previous findings[27,30,32,34,41]. It has to be noted that cecal tonsils provide protective immune response against bacterial and viral pathogens in the intestinal tract and any pathology associated with them would lead to adverse effects compromising the gut health.

It is observed most of the liver samples from IBD affected birds were normal and pathological changes may be associated with co-existing mycotoxicosis[34]. Contrary to this, in the current investigation liver changes were characteristic and consistent. Hemorrhages in proventriculus might be due to deficiency of clotting factors either linked to thrombocytopenia or related to Disseminated Intravascular Coagulopathy (DIC) or injury to blood vessel or secondary coagulation defect[42].

Ultrastructurally, thymus of IBD affected birds showed severe necrosis of the lymphocytes and hyperplasia of the reticular cells. Using SEM (Scanning Electron Microscopy) reduction in number and size of epithelial microvilli, gradual loss of the surface follicles and numerous epithelial erosions on the surface of the thymus has been recorded[43]. There are not many reports of thymic changes by previous workers. Lysosomes with remnants of necrotic lymphocytes, lipid vacuoles and myelin figure appearing as membrane bound electron dense aggregates within presumably large pale reticular cells (macrophages) is observed[44]. These cells were surrounded by degenerating lymphocytes in the early stages and pyroninophilic blast cells in the later part of the disease. Areas of lymphocytic apoptosis and engulfed phagocytic bodies within macrophages or macrophage like cells observed in the current study was indicative of high degree of apoptosis owing to viral interference. However, pyronophilic blast cells were not characteristic in the current investigation and viral particles were not detected in the lymphocytes as earlier reported[32]. In a recent study, it is explained that the granular discharge of BSDC that is predominantly glycoprotein contributes in transformation of these BSDC cells to macrophage like cells (Mal) in bursa that is experimentally infected IBD virus[45]. The virus particles single-shelled, non-enveloped virion with icosahedral symmetry and a diameter of around 50 nm were observed in negative staining preparations. These changes are in tune with the previous observations[32,44-47].

The RT-PCR was adopted for the detection of IBD antigen for amplification of 319 bp product corresponding to variable region of VP2 gene[48]. Presence of IBD virus was confirmed in 15 flock outbreaks. RT-PCR, targeting different regions of the IBD virus genome, including VP1, VP2 and VP4 genes, in concurrence with melting curve analysis is being investigated as a potential tool for molecular diagnosis of IBD[2,3,15-18]. In the recent years, the amplification of the VP2 gene has been a major focus. Amplicons of size 743 bp[16,49] and 474 bp[50] have been reported. However, recent study indicates loop-mediated isothermal amplification (LAMP) is 10 times more sensitive, specific and rapid compared to RT-PCR[11].

The amplicons obtained by PCR reaction of VP2 gene from samples IBD were subjected to sequence analysis and phylogenetic tree was drawn. Similarity in terms of percentage between various isolates was presented. This revealed 98 to 100% similarity of strain isolated in this study with Infectious Bursal Disease virus gene for VP5 protein and VP2-4-3 polyprotein, genomic RNA, IBD virus gene for polyprotein, mutant IBD virus strain AvvBvv segment A and other two Indian isolates. Also, the current isolate was distinct from various isolates of the world and formed a separate cluster with accession number X92760. Further the tree bifurcation suggested that the current isolate of the virus might have evolved phylogenetically among the X92760, MG489892 and AJ 318896 as common ancestor. The implications of the phylogenetic similarity and the impact on the strategies on disease control warrants further investigation.

Structural analysis of the IBD-VP2 protein using the SWISS PROT suggested that the VP2 of IBD was a manomeric protein with 99 amino acids. SWISS-PROT is a part of the UniProt Knowledgebase (UniProtKB), a protein sequence database that provides expert annotations on protein function, domain structure, and post-translational modifications, with very low redundancy. Of late, this has become a valuable resource for molecular biologists[51]. GMQE and QMEAND are Co global measurement that give an overall model quality measurement between 0 and 1, with higher numbers indicating higher expected quality. GMQE combines properties from the target-template alignment and the template structure. GMQE score of the IBD-VP2 was 0.07

suggesting that the optimum quality of the peptide in the current study[52]. SWISS-MODEL is a measure of how close the model was to structures of a similar size that were obtained experimentally[53,54]. Ramachandran plot results suggested the presence of the glycine like amino acids predominant in the alpha helical secondary structure of the protein[55]. The Ramachandran plot is a graphical representation used to visualize the allowed regions of amino acid residues in protein structures. Lately, it has become an essential tool for understanding protein conformation, validating structure models and also for studying secondary structure elements of proteins[56].

In the current investigation prevalence, age susceptibility, morbidity and mortality, clinical signs, gross pathology, concurrent infection, microscopic and ultrastructural Pathology and molecular confirmation by PCR and sequencing was studied in fifteen outbreaks of IBD. The gross and microscopic changes in bursa and lymphoid organs confirmed that IBDV targets the chicken's immune system in a very comprehensive and complex manner by destroying B lymphocytes and activation of macrophages. Areas of lymphocytic apoptosis and engulfed phagocytic bodies in these macrophages were observed in TEM. Phylogenetic tree for VP2 amplicons revealed 98 to 100% similarity with VP5 protein and VP2-4-3 polyprotein, genomic RNA, IBD virus gene for polyprotein, mutant IBD virus strain AvvBvv segment A and other two Indian isolates. Ramachandran plot suggested the presence of the glycine like amino acids predominant in the secondary structure of the protein.

Based on the various pathological and molecular investigations the immunosuppressive effects of IBD virus on health and in turn to the economy of poultry farming is clear and evident. Various other factors such as management, nutrition and climate change could also be involved in the expression of IBD in poultry. It is the utmost necessity to timely diagnose these conditions and control them effectively and more importantly educating the poultry farmers on timely implementation of vaccinations and biosecurity measures. Mitigating strategies involving epidemiological interventions, mechanistic studies on host immune responses, mutation based *in-silico* analysis of VP2 protein, enhanced diagnostics and making provision for better vaccines could be handy in addressing IBD in the future.

REFERENCES

1. Umar S, Munir M, U Ahsan I, Raza M, Chowdhury Z, Ahmed M and Shah. 2017. Immunosuppressive interactions of viral diseases in poultry. *World's Poult Sci J* **73:** 121-135.
2. Agnihotri AA, Awandkar SP, Kulkarni RC, Chavhan SG, Suryawanshi RD, Mohan A, Kulkarni M and Chavan VG. 2023. Isolation and molecular characterization of Infectious Bursal Disease virus circulating in western and central India. *Indian J Vet Res* **24:** 345-350.
3. Huang Y, Shu G, Huang C, Han J, Li J, Chen H and Chen Z. 2023. Characterization and pathogenicity of a novel variant Infectious Bursal Disease virus in China. *Front Microbiol*.
4. Tahir I and Alsayeqh AF. 2024. Phytochemicals: a promising approach to control infectious bursal disease. *Front Vet Sci*.
5. Gimeno IM and Schat KA. 2018. Virus-Induced Immunosuppression in Chickens. *Avian Dis* **62:** 272-285.
6. Jordan AB, Gongora V, Hartley D and Oura C. 2018. A review of eight high-priority, economically important pathogens of poultry within the Caribbean region. *J Vet Sci* **5:** 1-14.
7. Vandenberg T, Eterradossi N, Toquin D and Meulemans G. 2000. Infectious Bursal Disease (Gumboro disease). *Revue Sci Tech Office Intel Epiz* **19:** 527-543.
8. Qin Y and Zheng SJ. 2017. Infectious Bursal Disease Virus-Host Interactions: Multifunctional Viral Proteins that Perform Multiple and Differing Jobs. *Int J Mol Sci* **18:** 161-167.
9. Ingrao F, Rauw F, Lambrecht B and Vandenberg T. 2013. Infectious Bursal Disease: A complex host-pathogen interaction. *Dev Comp Immunol* **41:** 429-438.
10. Awandkar SP, Tembhurne PA, Kesharkar JA, Kurkure NV, Chaudhari SP, Bonde SW and Ingle VC. 2018. Identification and characterization of a novel Infectious Bursal Disease virus from outbreaks in Maharashtra Province of India. *Vet World* **11:** 1516-1525.
11. Dey S, Dinesh PC, Narayan R, Hemanta KM and Madhan MC. 2019. Infectious Bursal Disease virus in chickens: prevalence, impact and management strategies. *Vet Med Res Reports* **10:** 85-97.
12. Zachar T, Popowich S, Goodhope B, Knezacek T, Ojkic D, Willson P, Ahmed KA and Gomis S. 2016. A 5-year study of the incidence and economic impact of variant Infectious Bursal Disease viruses on broiler production in Saskatchewan, Canada. *Can J Vet Res* **80:** 255-261.
13. Sharma JM, Kim I, Rautenschlein S and Yeh H. 2000. Infectious Bursal Disease virus of chickens: Pathogenesis and immunosuppression. *Dev Comp Immunol* **24:** 223-235.
14. Luque D, Saugar I, Rejas MT, Carrascosa JL, Rodriguez JF and Caston JR. 2009. Infectious Bursal Disease virus: Ribonucleoprotein complexes of a Double-stranded RNA virus. *J Mol Biol* **386:** 891-901.
15. Vandenberg T, Morales D, Eterradossi N, Rivallan G, Toquin D, Raue R, Zierenberg K, Zhang M, Zhu Y and Wang C. 2004. Assessment of genetic, antigenic and pathotypic criteria for the characterization of IBDV strains. *Avian Pathol* **33:** 470-476.
16. Sreedevi B and Jackwood DJ. 2007. Real-Time Reverse Transcriptase-Polymerase Chain Reaction Detection and Sequence Analysis of the VP2 Hypervariable Region of Indian Very Virulent Infectious Bursal Disease Isolates. *Avian Dis* **51:** 750-757.
17. Wu CC, Rubinelli PA and Lin TL. 2007. Molecular detection and Differentiation of Infectious Bursal Disease Virus. *Avian Dis* **51:** 515-526.
18. Morla S, Deka P and Kumar S. 2016. Isolation of novel variants of Infectious Bursal Disease virus from different outbreaks in Northeast India. *Microb Pathog* **93:** 131-136.
19. Mendez F, Romero N, Cubas L, Laura DR, Dolores R and Rodriguez JF. 2017. Non-Lytic Egression of Infectious Bursal Disease Virus (IBDV) Particles from Infected Cells. *Plos One* **12:** 1-22.
20. Suvarna SK, Layton C and Bancroft JD. 2013. eds. Bancroft's theory and practice of histological techniques. Nottingham and Sheffield: Churchill Livingstone-Elsevier.
21. Barreto-Vieira DF and Barth OM. 2015. Eds. Microbiology in Agriculture and Human Health. Intech Open: London.

22. Karunakaran K, Thanappapilldi M and Raghavan N. 1993. Seroprevalence of Infectious Bursal Disease (IBD) in parts of Tamil Nadu, India. *Comp Immunol Microbiol Infect Dis* **16:** 241-244.
23. Farooq M, Durrani FR, Imran N, Durrani Z and Chand N. 2003. Prevalence and economic losses due to infectious Bursal diseases in broilers in Mirpur and Kotli district of Kashmir. *Int J Poult Sci* **2:** 267-270.
24. Preeti KS and Ramkaran LB. 2018. Histopathology of Bursa of Fabricius and postmortem findings in Infectious Bursal Disease affected broiler chickens in Haryana. *J Entomol Zool Stud* **6:** 876-879.
25. Mcilroy SG, Goodall EA and Mccracken RM. 1989. Economic effects of subclinical Infectious Bursal Disease on broiler production. *Avian Pathol* **18:** 465-480.
26. Zierenberg K, Nieper H, Vandenberg T, Ezeokoli C, Voss M and Muller H. 2000. The VP2 variable region of African and German isolates of Infectious Bursal Disease virus: Comparison with very virulent, classical virulent and attenuated tissue culture-adapted strains. *Arch Virol* **145:** 113-125.
27. Eterradossi N and Saif YM. 2008. Infectious Bursal Disease. In: Diseases of Poultry. Blackwell publishing, Ames, USA.
28. Linda OM, Michelle LK and Daral JJ. 2019. New introduction of a very virulent Infectious Bursal Disease virus in New York, USA. *Avian Pathol* **48:** 1-20.
29. Vandenberg TP. 2000. Acute Infectious Bursal Disease in poultry: a review. *Avian Pathol* **29:** 175-194.
30. Manjunath MT, Vijayasarathi SK, Sathyanarayana ML and Sreenivas Gowda RN. 2002. Comparative pathology of lymphoid organs in experimental Newcastle and infectious bursal disease. *Indian J Anim Sci* **72:** 1068-1071.
31. Preeti KS, Bai L, Ramkaran J, Naresh R and Gupta R. 2018. Epidemiological studies on Infectious Bursal Disease in broiler chickens in Haryana state during 2012-2015. *The Pharma Innovation J* **7:** 282-285.
32. Tanimura N, Tsukamoto K, Nakamura K, Narita M and Maeda M. 1995. Association between Pathogenicity of Infectious Bursal Disease Virus and Viral Antigen Distribution Detected by Immunohistochemistry. *Avian Dis* **39:** 9-20.
33. Sami WG and Baruah K. 1998. Pathology of Infectious Bursal Disease in broiler chickens. *Indian J Anim Sci* **68:** 1171-1172.
34. Singh J, Banga HS, Brar RS, Singh ND, Sodhi S and Leishangthem GD. 2015. Histopathological and immunohistochemical diagnosis of Infectious Bursal Disease in poultry birds. *Vet World* **8:** 1331-1339.
35. Cosgrove AS. 1962. An apparently new disease of chickens avian nephrosis. *Avian Dis* **6:** 385-389.
36. Gowthaman V, Sing SD, Dhama K, Barathidasan R and Anjaneya BP. 2012. Infectious Bursal Disease (IBD) playing a triggering role in *E. Coli* and mycoplasma induced respiratory disease complex in broilers. *Vet Pract* **13:** 223-225.
37. Devigasri C, Sankar S, Niranjana S, Rajalakshmi, Nair A and Mini M. 2018. Concurrent infection of Infectious Bursal Disease and pseudomoniasis in poultry - A Case Study. *Int J Sci Environ Technol* **7:** 1777-1781.
38. Mekibib B, Abera M, Mekuria S, Farooq UB and Abebe R. 2018. Clinicopathological Features of Concurrent Outbreak of Gumboro Disease and Aspergillosis in Chicken in Hawassa City, Ethiopia. *Asian J Poult Sci* **12:** 25-30.
39. Islam MR, Chowdhury EH, Das PM and Dewan ML. 1997. Pathology of acute Infectious Bursal Disease in chickens induced experimentally with a very virulent virus isolate. *Indian J Anim Sci* **67:** 7-9.
40. Islam NU, Saleemi MK, Khan MZ, Butt SL, Khan A, Javed I, Awan FS and Rafique S. 2013. Molecular diagnosis and pathology of chicken infectious anemia in commercial white leghorn layer flocks in Pakistan. *Vet J* **33:** 378-381.
41. Singh MP, Singh A, Grewal GS and Oberoi MS. 2002. Clinico-pathological studies of field isolates of Infectious Bursal Disease in broiler chicks. *Indian J Anim Sci* **72:** 38-41.
42. Zeryehun T, Hair-Bejo M and Rasedee A. 2012. Hemorrhagic and clotting abnormalities in Infectious Bursal Disease in specific pathogen free chick. *World Appl Sci J* **16:** 1123-1130.
43. Naqi SA and Millar DL. 1979. Morphologic changes in the Bursa of Fabricius of chickens after inoculation with Infectious Bursal Disease virus. *Am J Vet Res* **40:** 1134-1139.
44. Cheville NF. 1967. Studies on the pathogenesis of Gumboro disease in the Bursa of Fabricius, spleen and thymus of the chicken. *Am J Pathol* **51:** 527-551.
45. Felfoldi B, Bodi I, Minko K, Benyeda Z, Nagy N, Magyar A and Olah I. 2021. Infection of bursal disease virus abrogates the extracellular glycoprotein in the follicular medulla. *Poult Sci Apr* **100:** 101-000.
46. Kaufer I and Weiss E. 1976. Electron-microscope studies on the pathogenesis of Infectious Bursal Disease after intrabursal application of the causal virus. *Avian Dis* **20:** 483-95.
47. Christopher DS, Minnie M, Peter AB, Anbumani SP, Doraiswami J, Rajendran MP and Murugan M. 1997. An outbreak of acute Infectious Bursal Disease in poultry: Ultrastructural studies on bursa from clinical cases. *Indian J Anim Sci* **67:** 563-564.
48. Kong LL, Omar AR, Bejo MH, Ideris A and Tab SW. 2009. Development of SYBR green I based one-step real-time RT-PCR assay for the detection and differentiation of very virulent and classical strains of Infectious Bursal Disease virus. *J Virol Meth* **161:** 271-279.
49. Kim HR, Kwon YK, Bae YC, Oem JK and Lee OS. 2010. Genetic characteristics of virion protein 2 genes of Infectious Bursal Disease viruses isolated from commercial chickens with clinical disease in South Korea. *Poult Sci* **89:** 1642-1646.
50. Ghorashi SA, Orourke D, Ignjatovic J and Noormohammadi AH. 2011. Differentiation of Infectious Bursal Disease virus strains using real-time RT-PCR and high resolution melt curve analysis. *J Virol Methods* **171:** 264-271.
51. UniProt Consortium. 2023. UniProt: Universal Protein Knowledgebase in 2023. *Nucl Acids Res* **51:** D523-D530.
52. Mariani V, Biasini M, Barbato A and Schwede T. 2013. LDDT: a local superposition-free score for comparing protein structures and models using distance difference tests. *Bioinform* **29:** 2722-2728.
53. Studer G, Rempfer C, Waterhouse AM, Gumienny R, Haas J and Schwede T. 2020. Qmeandisco - distance constraints applied on model quality estimation. *Bioinform* **36:** 1765-1771.
54. Benkert P, Biasini M and Schwede T. 2011. Toward the estimation of the absolute quality of individual protein structure models. *Bioinform* **27:** 343-350.
55. Chenn VB, Arendall WB, Headd JJ, Keedy DA, Immormino RM, Kapral GJ, Murray LW, Richardson JS and Richardson DC. 2010. All-atom structure validation for macromolecular crystallography. *Acta Cryst D* **66:** 16-21.
56. Ramachandran GN and Sasisekharan V. 1968. Conformation of polypeptides and proteins. *Adv Protein Chem* **23:** 283-438.